Supplementary Figures

Title:
Linker mutations dissociate the function of synaptotagmin I during evoked and spontaneous release and reveal membrane penetration as a step during excitation-secretion coupling

Authors:
Huisheng Liu[1,2,4], Hua Bai[1,4], Renhao Xue[1], Hirohide Takahashi[3], J. Michael Edwardson[3] & Edwin R. Chapman[1]

[1]Howard Hughes Medical Institute and Department of Neuroscience, University of Wisconsin, Madison, Wisconsin, USA.
[2]Present address: Waisman Center, University of Wisconsin, Madison, Wisconsin, USA.
[3]Department of Pharmacology, University of Cambridge, Cambridge, United Kingdom
[4]These authors contributed equally to this work.
Correspondence should be addressed to E.R.C. (chapman@wisc.edu)

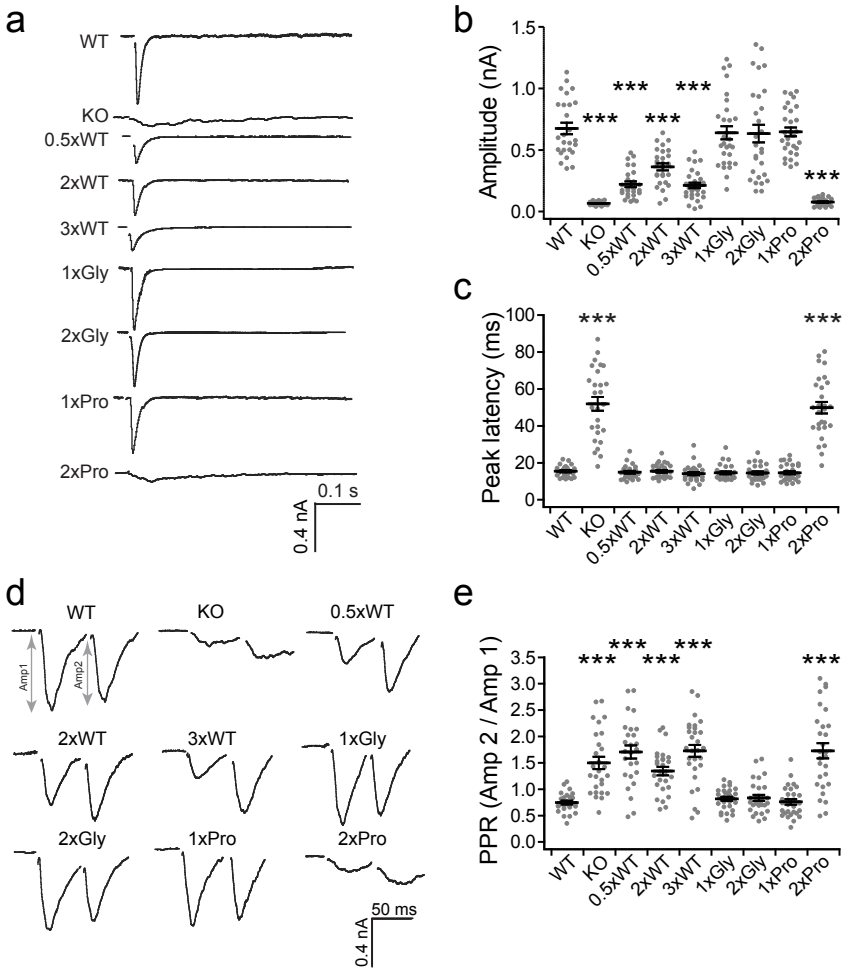

Supplementary Figure 1. The experiments in Fig. 2a, b, d and 3a, b were repeated at 2 mM $[Ca^{2+}]_o$. (a) Representative eEPSC traces recorded from WT, syt KO, and KO neurons that expressed each linker mutant. (b, c) Scatter plots of single eEPSC amplitudes (b) and latencies to peak (c). (d) Representative eEPSCs recorded in paired-pulse experiments with 50 ms inter-stimulus intervals. (e) Scatter plot of the PPRs, calculated as in Fig. 3. For each condition, we recorded from 26 - 29 cells from a total of six coverslips, where two coverslips were obtained from each of three independent litters of mice. The mean values ± SEM are indicated. Bootstrap statistical analysis was carried out, and the results are provided in Supplementary Statistics. Asterisks indicate differences compared with WT; *** $p < 0.001$.

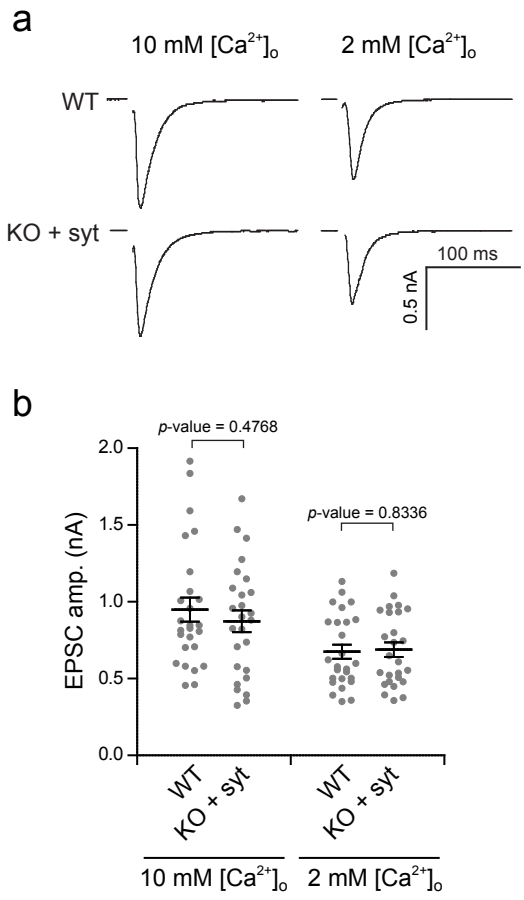

Supplementary Figure 2. Re-expression of syt fully rescues normal synaptic transmission in syt KO neurons. (a) Representative eEPSC traces recorded from WT neurons, and syt KO neurons that expressed WT syt cDNA, in the presence of 10 or 2 mM $[Ca^{2+}]_o$. (b) Scatter plots of the individual eEPSC amplitudes. For each condition, we recorded from 26 cells from a total of six coverslips, where two coverslips were obtained from each of three independent litters of mice. The mean values ± SEM are indicated. P-values, determined using a bootstrap approach, are indicated.

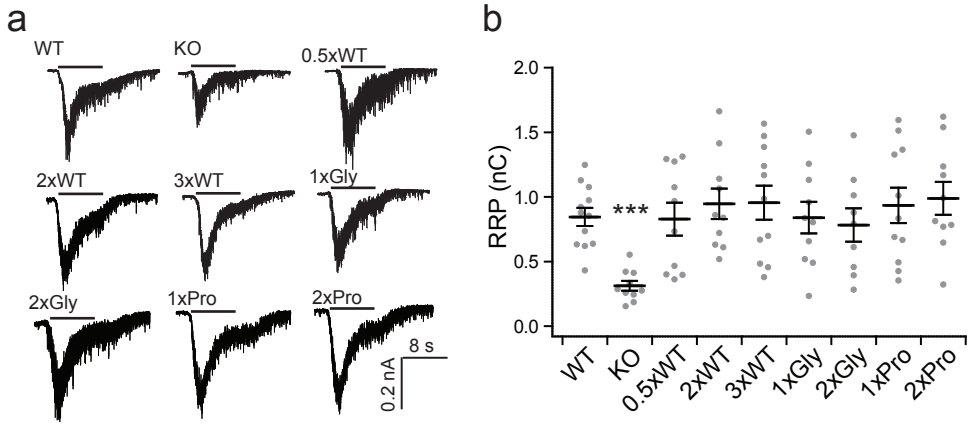

Supplementary Figure 3. Syt linker mutants rescue the size of the RRP in syt KO neurons. (a) Example EPSCs in response to a pulse of hypertonic sucrose (500 mM) for 8 s. (b) Scatter plot of the total transfer charge upon exposure to sucrose; all of the syt linker mutants fully rescued the diminished size of the RRP in the KO. For each condition we recorded from 9 - 12 neurons from a total of three coverslips; each coverslip was derived from an independent litter of mice. The mean values ± SEM are indicated. Statistical significance was determined using a bootstrap approach; no significant differences among neurons expressing each of the linker mutants, only the KO had alterations in the RRP; detailed analysis is provided in Supplementary Statistics. Asterisks indicate differences compared with WT; *** $p < 0.001$.

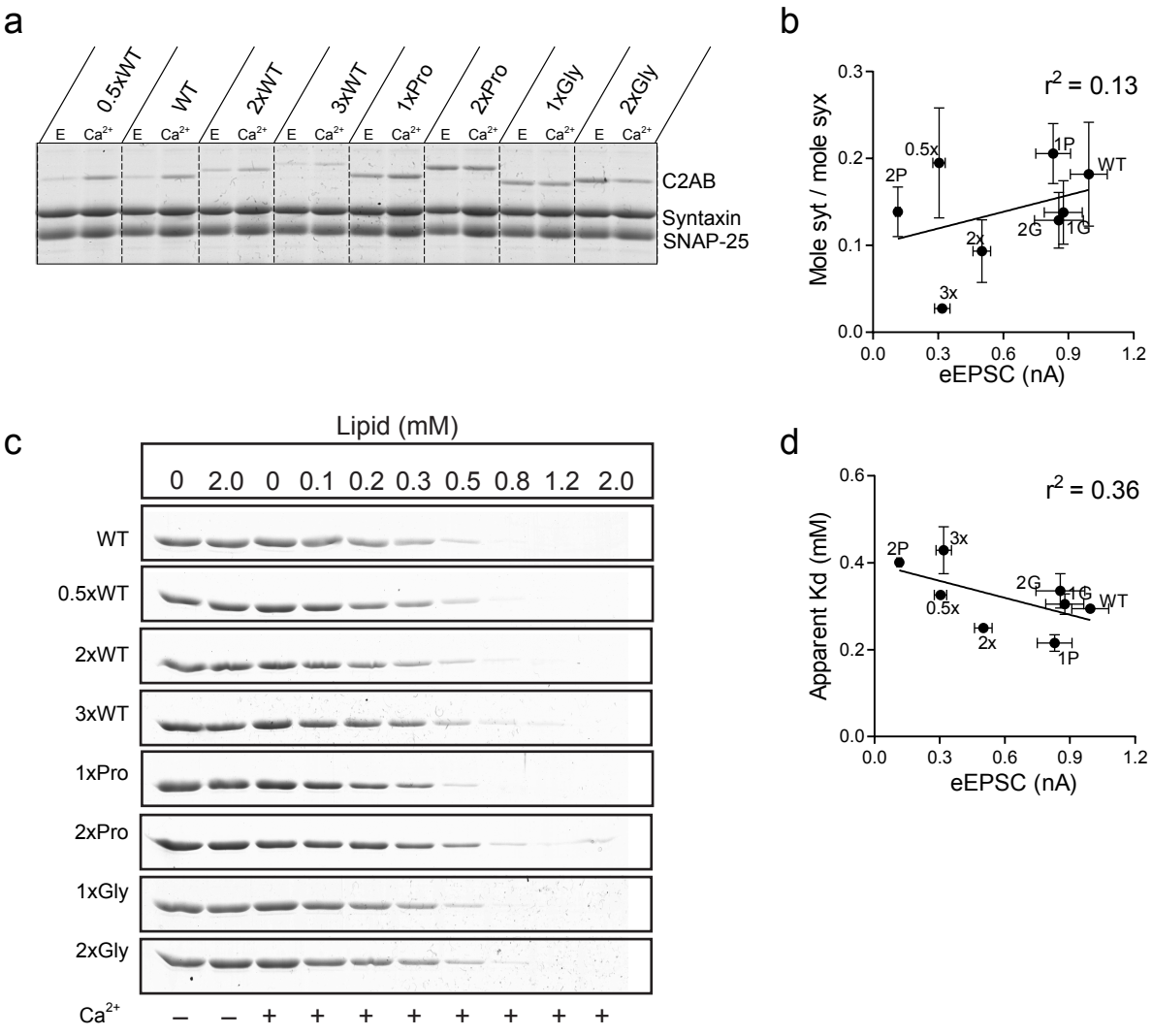

Supplementary Figure 4. Correlation plots of syt linker mutant t-SNARE or PS binding activity versus evoked transmission. (a) t-SNARE binding activity (defined as the mole of syt bound per mole of syntaxin (syx)) of WT or linker mutant cytoplasmic domains (C2AB) was measured using a co-flotation assay. The final $[Ca^{2+}]_{free}$ was 1 mM; [EGTA] was 0.2 mM. Four independent experiments were carried out. (b) t-SNARE binding activity of WT or linker mutant forms of C2AB were plotted versus eEPSC amplitude from Fig. 2b. (c) Binding of WT or linker mutant forms of C2AB to PS-bearing liposomes was monitored using a co-sedimentation assay; depletion of the supernatant was monitored via SDS-PAGE and staining with Coomassie blue (the staining intensity reflects free C2AB in the supernatant), and these data were used to calculate the amount of bound material, in the absence (–; 0.2 mM EGTA) or presence (+) of 1 mM $[Ca^{2+}]_{free}$. Three independent experiments were carried out. (d) PS binding activity (defined as the apparent Kd for lipid; note that [lipid] and not [liposome] values were used, thus resulting in apparent Kd values in the mM range) of WT or linker mutants were plotted versus the eEPSC values that were, again, from Fig. 2b; error bars represent SEM. Equations and p-values for the linear regressions are listed in Supplementary Statistics. For clarity, the upper and lower portions of each gel (i.e. regions lacking proteins), were cropped.

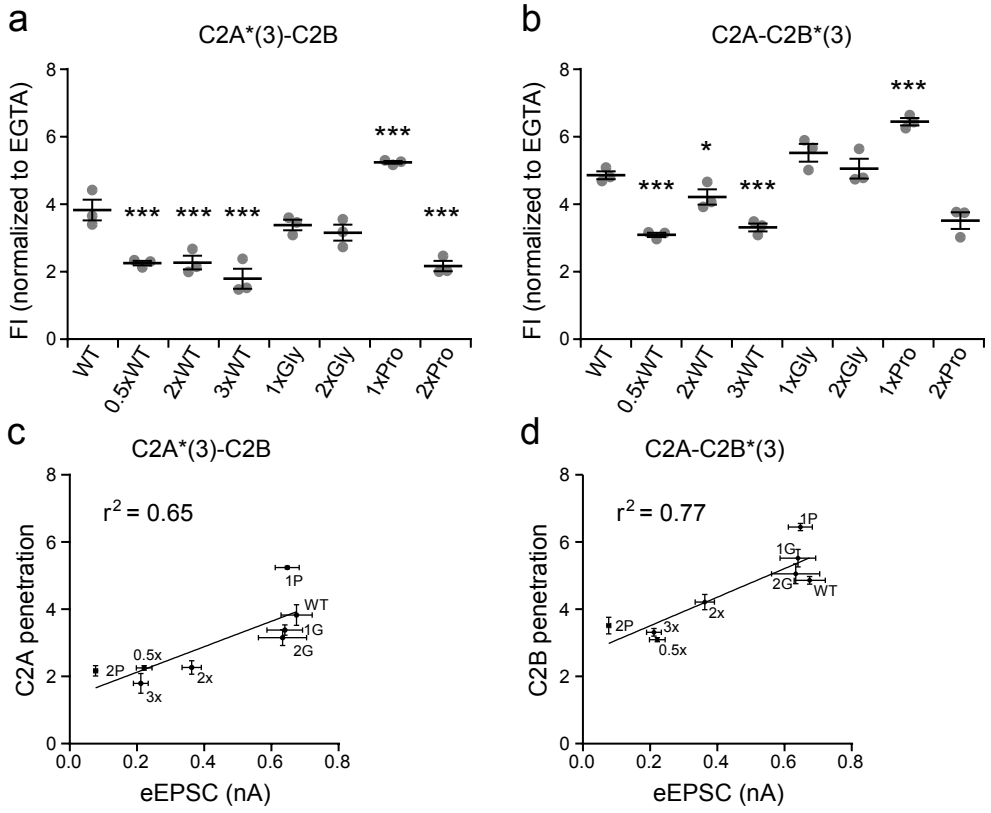

Supplementary Figure 5. Positive correlation between the membrane penetration activity of WT and mutant forms of syt and eEPSC amplitude at a lower concentration of Ca^{2+}. (a - b) Scatter plots of peak values of the normalized NBD fluorescence of C2A*(3)-C2B (a) and C2A-C2B*(b) in 100 µM Ca^{2+}, using liposomes that harbored 25% PS. For each condition, 3 independent experiments were carried out. (c, d). Positive correlation between the membrane penetration activity of C2A (c), and C2B (d), and eEPSC amplitude recorded at 2 mM $[Ca^{2+}]_o$, taken from Supplemental Fig. 1b. The mean values ± SEM are indicated. Statistical significance was determined using a bootstrap approach. Asterisks indicate differences compared with WT; * $p < 0.05$, *** $p < 0.001$. Detailed statistical analysis, and the equations and p-values for the linear regressions, are provided in Supplementary Statistics.

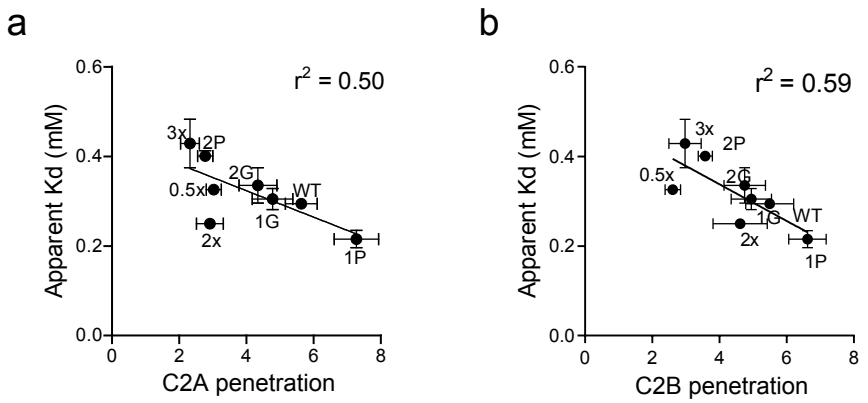

Supplementary Figure 6. Partial correlation between the PS binding and membrane penetration activity of linker mutant forms of syt. Penetration data from Fig. 4 were plotted versus the apparent affinities for binding membranes from Supplementary Fig. 4d; penetration data for C2A and C2B are shown in panel a and b, respectively; error bars represent SEM. Equations and p-values for the linear regressions are provided in Supplementary Statistics.

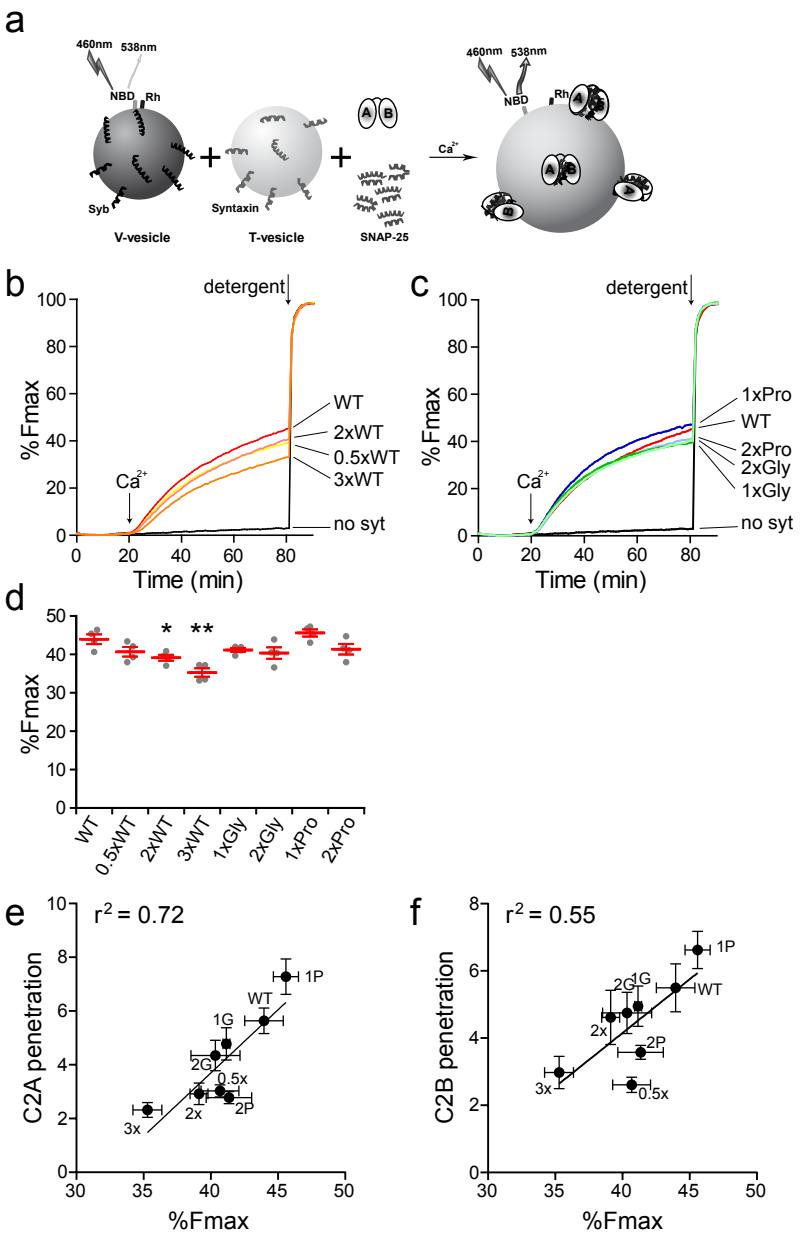

Supplementary Figure 7. Correlation between membrane penetration activity and the ability of syt linker mutants to drive Ca^{2+}-triggered lipid mixing in a reconstituted membrane fusion assay. (a) A schematic diagram of the reconstituted fusion system; the donor (NBD) fluorescence increases, due to dequenching, upon fusion. (b, c) Representative traces of reconstituted membrane fusion reactions regulated by WT or linker mutant forms of syt; the arrow indicates the addition of Ca^{2+} (1 mM free). (d) Scatter plot of the extent of fusion 1 h after addition of Ca^{2+} For each condition, four independent experiments were carried out. (e, f) Positive correlation between membrane penetration of loop 3 in either C2A or C2B, taken from Fig. 4c,f, with the extent of fusion. Plotted values represent the mean ± SEM. Statistical significance was determined using a bootstrap approach. Asterisks indicate differences compared with WT; * $p < 0.05$, ** $p < 0.01$. Detailed statistical analysis, and equations and p-values for the linear regressions, are provided in Supplementary Statistics.

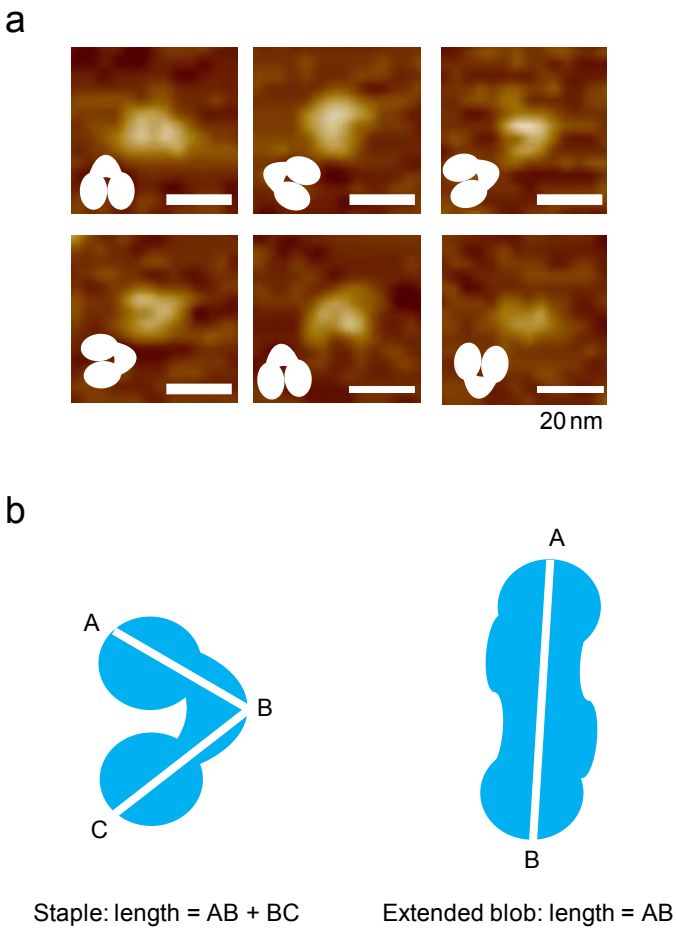

Supplementary Figure 8. WT C2AB adopts a horseshoe shaped structure. (a) Schematic representations of the horseshoe structures in the AFM images shown in Fig. 5a. (b) Illustration of the method used to determine the lengths of horseshoe structures and extended blobs.

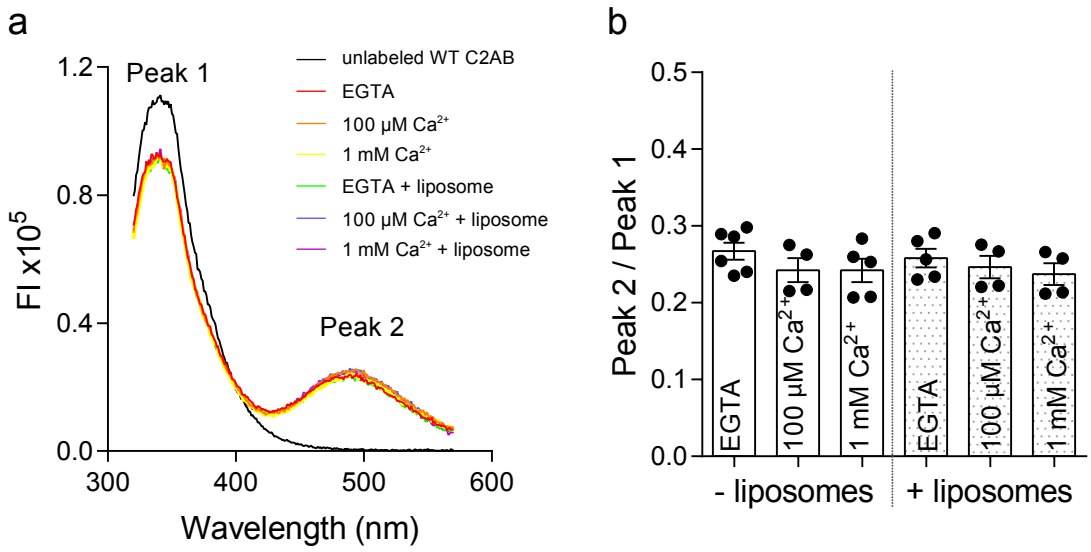

Supplementary Figure 9. FRET measurements revealed that the intramolecular interaction between C2A and C2B is not influenced by either Ca^{2+} or membranes. (a) Representative emission spectra of AEDANS-labeled C2AB in 0.1 mM EGTA, 0.1 or 1 mM free Ca^{2+} with, or without, liposomes that harbored 25% PS; the labeled protein was excited at 295 nm. Peak 1 is the emission peak of two native Trp residues in C2B domain. Peak 2 is the emission peak of AEDANS conjugated to the C2A domain. As a control, unlabeled C2AB was analyzed in parallel (in EGTA, minus liposomes). (b) Scatter plot of peak 2 divided by peak 1, under each condition; plotted values represent the mean ± SEM. For each condition, 4 - 6 independent experiments were carried out. Statistical significance was determined using a bootstrap approach; no differences were observed (Supplementary Statistics).

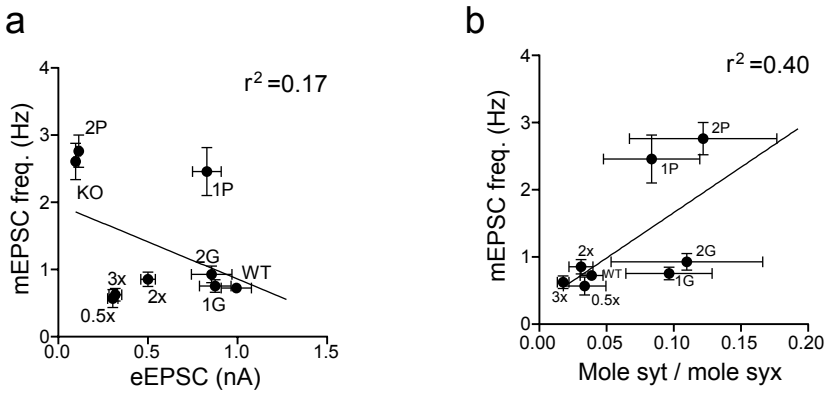

Supplementary Figure 10. Correlation analysis of mEPSC frequency. (a) Lack of correlation between the ability of the syt linker mutants to regulate evoked versus spontaneous release. Data for mEPSCs and eEPSCs are from Fig. 6d and Fig. 2b, respectively. (b) Correlation plot of the ability of the syt linker mutants to suppress spontaneous release, and to bind t-SNAREs in the absence of Ca^{2+}. Data for mEPSCs are from Fig. 6d and Ca^{2+}-independent t-SNARE binding activity was obtained from Supplementary Fig. 4a. Plotted values represent the mean ± SEM. Equations and p-values for the linear regressions are listed in Supplementary Statistics.